

PAPER • OPEN ACCESS

Influence of the electromagnetic fields on hadronic observables in proton-induced collisions

To cite this article: L. Oliva *et al* 2020 *J. Phys.: Conf. Ser.* **1667** 012032

View the [article online](#) for updates and enhancements.

You may also like

- [Scaling behaviours of the \$p_T\$ spectra for identified hadrons in \$pp\$ collisions](#)
W C Zhang
- [The Forward Physics Facility at the High-Luminosity LHC](#)
Jonathan L Feng, Felix Kling, Mary Hall Reno et al.
- [Ultradense protium \$p\(0\)\$ and deuterium \$D\(0\)\$ and their relation to ordinary Rydberg matter: a review](#)
Leif Holmlid and Sindre Zeiner-Gundersen



Breath Biopsy[®] OMNI[®]

The most advanced, complete solution for global breath biomarker analysis

TRANSFORM YOUR
RESEARCH WORKFLOW



Expert Study Design
& Management



Robust Breath
Collection



Reliable Sample
Processing & Analysis



In-depth Data
Analysis



Specialist Data
Interpretation

Influence of the electromagnetic fields on hadronic observables in proton-induced collisions

L. Oliva^{1,2}, P. Moreau², V. Voronyuk^{3,4} and E. Bratkovskaya^{1,2}

¹ GSI Helmholtzzentrum für Schwerionenforschung GmbH, Darmstadt, Germany

² Institut für Theoretische Physik, Goethe-Universität, Frankfurt am Main, Germany

³ Joint Institute for Nuclear Research, Dubna, Moscow region, Russia

⁴ Bogolyubov Institute for Theoretical Physics, Kiev, Ukraine

E-mail: oliva@fias.uni-frankfurt.de

Abstract. We investigate proton-gold collisions at top RHIC energy $\sqrt{s_{NN}} = 200$ GeV within the Parton-Hadron-String Dynamics (PHSD) approach, focusing on the influence of the electromagnetic fields on final hadronic observable. We discuss the space-time distribution of the magnetic and electric field components, showing that the electric field E_x along the impact parameter direction is comparable in magnitude to the magnetic field B_y perpendicular to the reaction plane. We discuss the effect of these fields on the directed flow v_1 of pions and kaons. While there is no visible effect of electromagnetic fields in 5% central collisions, the result for collisions at fixed impact parameter clearly indicates an electromagnetically-induced splitting in the v_1 of positively and negatively charged mesons; the effect, driven by the huge E_x component, is larger for kaons than to pions and increases with the impact parameter of the collision.

1. Introduction

The recent experimental and theoretical results on high-multiplicity events in small systems, such as proton-proton and proton-nucleus collisions, seems to indicate the formation of short-lived droplets of Quark-Gluon Plasma (QGP) [1], which give rise to final-state momentum anisotropies comparable in magnitude to those found in collisions between two heavy ions. Among the Fourier coefficients of the particle azimuthal distribution the directed flow v_1 , which refers to a collective sideways deflection of particles, is a promising probe for the electromagnetic fields (EMF) produced in the collision [2, 3, 4]. Indeed, extremely intense magnetic fields are produced in non-central relativistic heavy-ion collisions mainly due to the motion of spectator charges [5, 6, 10], with a maximum magnitude at top RHIC and LHC energies of about $|eB_y| \sim 5-50 m_\pi^2$, corresponding to $\sim 10^{18} - 10^{19}$ Gauss. In asymmetric systems, along with the magnetic field perpendicular to the reaction plane B_y , a huge electric field along the impact parameter axis E_x is formed mainly due to the different number of protons in the two nuclei. Focusing on p+Au collisions at RHIC energy of $\sqrt{s_{NN}} = 200$ GeV, we perform simulations with the Parton-Hadron-String Dynamics (PHSD) off-shell transport approach, which describes the full space-time evolution of a relativistic nuclear collision [7, 8, 9] and includes also the dynamical EMF [6, 2]; we investigate their effect on the collective behaviour of the created matter, quantifying in particular the charge-dependent directed flow of the most abundant hadron species at top RHIC energy [11].



2. Remainder of the PHSD model

The Parton-Hadron-String Dynamics (PHSD) approach is a covariant dynamical model for strongly interacting particles whose time evolution, both in the partonic and in the hadronic phase, is governed by off-shell transport equations, which are derived from the Kadanoff-Baym equations for non-equilibrium Green functions [7, 8]. Primary nucleon-nucleon scatterings between the two colliding nuclei lead to the formation of color-neutral strings which fragment into “pre-hadrons”, i.e., baryons and mesons within their formation time (taken to be 0.8 fm/c in their rest frame). If the local energy density is above the critical value for the deconfinement transition pre-hadrons dissolve in massive quarks, antiquarks and gluons plus a mean-field potential. The Dynamical Quasi-Particle Model (DQPM) [8] defines the parton spectral functions (i.e. masses and widths) and the self-generated mean-field potentials, whose parameters are determined fitting the lattice QCD thermodynamics. The transition from partonic to hadronic degrees of freedom is described by dynamical hadronization, modeled through covariant transition rates for the fusion of off-shell partons to off-shell hadronic states [8, 9].

PHSD includes the dynamical formation and evolution of the retarded EMF and its influence on quasi-particle as well as the back-reaction of particle dynamics on the fields [2, 6, 10]; indeed, the off-shell transport equation are supplemented by the Maxwell equations for the electric field \mathbf{E} and the magnetic field \mathbf{B} . Neglecting terms which depend on the acceleration of the charge and considering that in a nuclear collision the total fields are a superposition of the fields generated from all moving charges, one obtains the following expressions for the electric and magnetic fields:

$$e\mathbf{E}(\mathbf{r}, t) = \sum_i \frac{\text{sgn}(q_i)\alpha_{em}\mathbf{R}_i(t)(1 - \beta_i^2)}{\left\{[\mathbf{R}_i(t) \cdot \boldsymbol{\beta}_i]^2 + R_i(t)^2(1 - \beta_i^2)\right\}^{3/2}}, \quad (1)$$

$$e\mathbf{B}(\mathbf{r}, t) = \sum_i \frac{\text{sgn}(q_i)\alpha_{em}\boldsymbol{\beta}_i \times \mathbf{R}_i(t)(1 - \beta_i^2)}{\left\{[\mathbf{R}_i(t) \cdot \boldsymbol{\beta}_i]^2 + R_i(t)^2(1 - \beta_i^2)\right\}^{3/2}}, \quad (2)$$

where the sum over i runs over all particles with charge q_i , velocity $\boldsymbol{\beta}_i$ and position \mathbf{r}_i ; $\alpha_{em} = e^2/4\pi \simeq 1/137$ is the electromagnetic fine-structure constant and $\mathbf{R}_i = \mathbf{r} - \mathbf{r}_i$. The quasiparticle propagation in the electromagnetic field is determined by the Lorentz force $\mathbf{F}_i = q_i(\mathbf{E} + \boldsymbol{\beta}_i \times \mathbf{B})$.

3. Space-time distributions of electromagnetic field

In p+Au collisions the initial EMF do not depend significantly on the impact parameter b , since they correspond mainly to the fields produced by the gold nucleus moving at velocity close to the speed of light. Nevertheless, the point in which the proton hits the gold nuclei has a strong impact on the field magnitude filled by it. In Fig. 1 we show the time evolution of the fields E_x (*left panels*) and B_y (*right panels*) produced at top RHIC energy in p+Au collisions at $b = 4$ fm. We see that the electric field is strongly asymmetric inside the overlap area, where for collision at $b = 4$ fm both $|eB_y|$ and $|eE_x|$ reaches values $\simeq 2m_\pi^2$, while the other electromagnetic field components are close to zero. From the different lines we can see how the maximum values of $|E_x|$ and $|B_y|$ changes moving in the transverse plane respect to the centre of the overlap area $\{x, y\} = \{2 \text{ fm}, 0 \text{ fm}\}$. For what concern the temporal evolution, both $|B_y|$ and $|E_x|$ decrease very fast, approaching zero after ~ 0.25 fm/c from the first nucleon-nucleon collisions corresponding to $t = 0$ fm/c. While moving in the x -direction the value of $|E_x|(x, 0, 0)$ and $|B_y|(x, 0, 0)$ changes of about 20-25% in 1 fm, spanning the y -direction $|E_x|(2, y, 0)$ and $|B_y|(2, y, 0)$ remain almost homogeneous in a region of at least 6 fm. Hence, for non-central collisions there is a wide area around the point where the proton hits the nucleus in which not only the magnetic field but also the electric field is intense, even though they last only for a small fraction on fm/c [11].

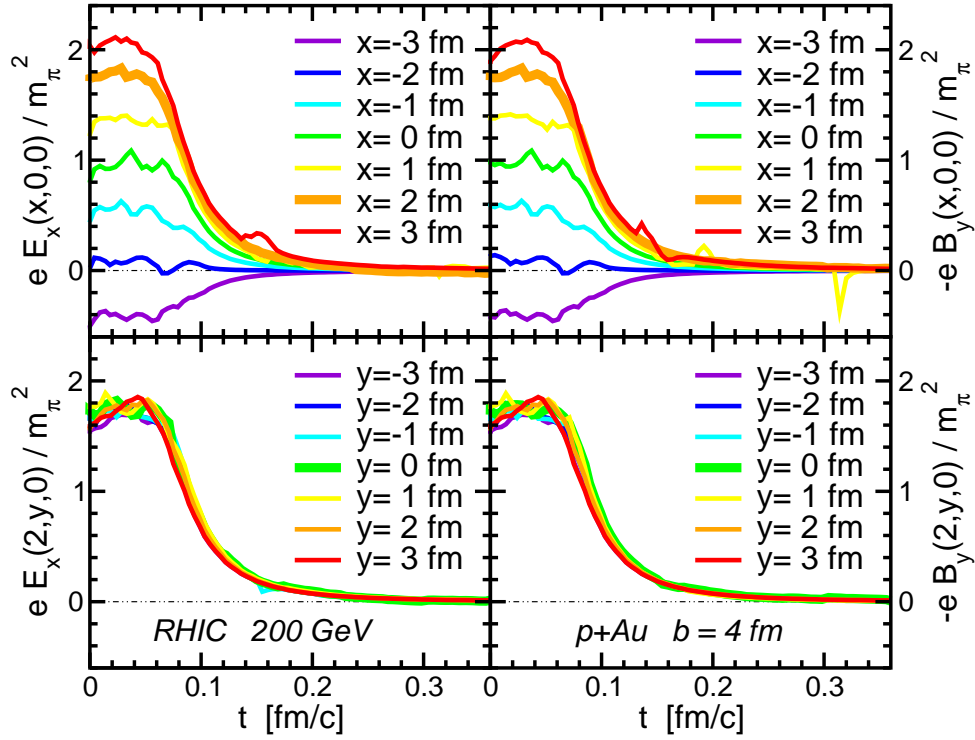


Figure 1. Time evolution of the event-averaged electromagnetic field components E_x (left panels) and B_y (right panels) for p+Au collisions at $\sqrt{s_{NN}} = 200$ GeV with impact parameter $b = 4$ fm. The different lines correspond to different values of $x \in [-3, 3]$ fm at $y = z = 0$ fm (upper panels) and different values of $y \in [-3, 3]$ fm at $x = b/2 = 2$ fm and $z = 0$ fm (lower panels).

4. Directed flow

The first Fourier coefficient of the azimuthal particle distribution is the directed flow

$$v_1^{\{\Psi_1\}} = \langle \cos[\phi - \Psi_1] \rangle / \text{Res}(\Psi_1), \quad (3)$$

where ϕ is the azimuthal angle of the particle and the brackets indicate average over all events; $v_1^{\{\Psi_1\}}$ takes into account the first-order event-plane angles Ψ_1 computed in each event and the event-plane angle resolution $\text{Res}(\Psi_1)$ determined by means of the three-subevent method [12]. The directed flow is a very promising observable to investigate the influence of EMF, since it could lead to a separation of positively and negatively charged particles along the impact parameter axis. In Fig. 2 we plot the rapidity dependence of $v_1^{\{\Psi_1\}}$ of π^+ (solid blue line), π^- (dashed red line), K^+ (solid green line) and K^- (dashed orange line) for 5% central p+Au collisions at $\sqrt{s_{NN}} = 200$ GeV computed with PHSD including the EMF dynamics; the event-plane angle Ψ_1 is computed in the pseudorapidity range $-4 < \eta < -3$ where the resolution is $\text{Res}(\Psi_1^{-4 < \eta < -3}) \simeq 0.293$. Within the present statistics, in simulations of 5% most central p+Au collisions, there is no visible difference in this observable between the positively and negatively charged particle of the same species. This could be due to the following reasons. From one hand, the multiplicity fluctuations in the final state mixes events from different impact parameters. From the other hand, the weak correlation in experiments and in “minimum bias” simulations between the event plane Ψ_1 respect to which the directed flow is computed and the reaction plane defined by the beam axis and the impact parameter direction leads to a cancellation, at least partial, of opposite contributions in the directed flow.

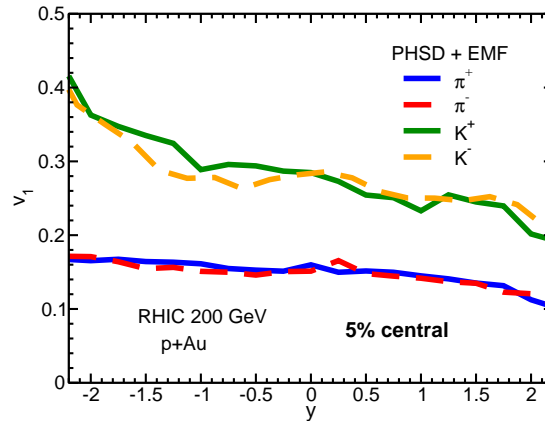


Figure 2. Directed flow of identified particles, π^+ , π^- , K^+ and K^- , as a function of rapidity for 5% central p+Au collisions at $\sqrt{s_{NN}} = 200$ GeV obtained with PHSD simulations with EMF.

For a deeper investigation we have performed simulations of $\sqrt{s_{NN}} = 200$ GeV p+Au collisions at fixed impact parameter ($b = 2$ fm and $b = 6$ fm) and computed the directed flow simply by means of $v_1 = \langle \cos \phi \rangle$, namely computing v_1 respect to the true reaction plane. The results for pions and kaons (in percentage) are shown in Fig. 3 as a function of rapidity. Simulations with and without the inclusion of EMF are labelled by solid and dashed curves respectively. Firstly, we focus on the left panels where the directed flow of π^+ (blue lines) and π^- (red lines) is plotted. Within simulations without EMF the two oppositely-charged pions have very similar v_1 . Switching on the EMF in the PHSD simulations, we find that π^+ and π^- are pushed by the EMF along the positive and negative x -direction respectively, therefore leading to a splitting in the v_1 of the two particles. Moreover, by comparing the results at $b = 2$ fm and $b = 6$ fm we see that the effect is bigger for higher impact parameters. For what concern kaons, as shown in the right panels, the EMF generate a flip in the directed flow of K^+ (green lines) and K^- (orange lines). Indeed, the two mesons present a different v_1 even in simulations that do not account for the EMF, since K^+ receive more contributions from u and d quarks coming from the initial colliding nuclei with respect to K^- ; hence, at backward rapidity the v_1 of K^+ is smaller than that of K^- [13]. The electromagnetically-induced splitting in the directed flow of charged kaons is turned over respect to that discussed above and dominates over it. The direction of the splitting in the directed flow of both meson species results from the balance between sideways deflections on charged particles by the electric and magnetic part of the Lorentz force: according to our convention for the reference frame, the electric force pushes positively charged particles along the positive x -direction and negatively charged particles along the negative x -direction while the magnetic force push charged particles in the other way around [2, 3, 4, 10]. The arrows in Fig. 3 highlight that the winner of this force balance in proton-nucleus reactions is the electric field. See Ref. [11] for more details on the electromagnetically-induced splitting of the directed flow of pions and kaons and for the identification of the contributions coming from the partonic and hadronic stages of the collision.

5. Conclusions

In this work we have studied p+Au collisions at $\sqrt{s_{NN}} = 200$ GeV with the PHSD approach, which describes the entire dynamical evolution of the collision and includes in a consistent way the dynamical generation of retarded electromagnetic fields (EMF) and their influence on quasi-particle propagation. We have shown the time evolution of the transverse components of the field: the electric field along the impact parameter axis E_x is comparable in magnitude to

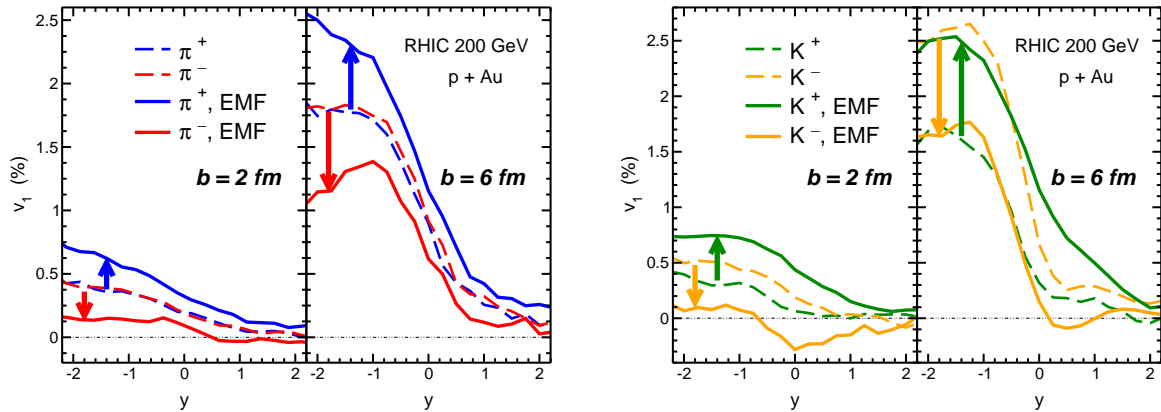


Figure 3. Directed flow of pions (*left panels*) and kaons (*right panels*) as a function of rapidity for $b = 2$ fm and $b = 6$ fm p+Au collisions at $\sqrt{s_{NN}} = 200$ GeV obtained with PSHD simulations with (solid curves) and without (dashed curves) EMF.

the magnetic field perpendicular to the reaction plane B_y ; both field components are strongly asymmetric inside the overlap region and decrease very fast, approaching zero after about 0.25 fm/c from the first nucleon-nucleon collision. Through a comparison of PHSD simulations with and without the inclusion of the EMF we have identified the impact of these fields on final observables: the EMF can modify the final distributions of particles with the same mass but opposite electric charge and we have clearly seen this effect in the directed flow of pions and kaons in p+Au collisions at fixed impact parameter. The v_1 of π^+ and K^+ is pushed upward and the v_1 of π^- and K^- is pushed downward with respect to the result without EMF. This splitting is more pronounced in the Au-going side and increases for more peripheral collisions.

Acknowledgments

The authors acknowledge fruitful discussions with W. Cassing, D. McGlinchey, I. Selyuzhenkov, O. Soloveva, T. Song and Q. Xu. L.O. and E.B. acknowledge support by the Deutsche Forschungsgemeinschaft (DFG) through the grant CRC-TR 211 'Strong-interaction matter under extreme conditions' and from the COST Action THOR, CA15213. L.O. has been in part supported by the Alexander von Humboldt Foundation. The computational resources have been provided by the LOEWE-Center for Scientific Computing and the Green Cube at GSI.

References

- [1] Aidala C *et al.* [PHENIX Collaboration] (2019) *Nature Phys.* **15** 214
- [2] Voronyuk V, Toneev V D, Voloshin S A and Cassing W (2014) *Phys. Rev. C* **90** 064903
- [3] Gursoy U, Kharzeev D and Rajagopal K (2014) *Phys. Rev. C* **89** 054905
- [4] Das S K, Plumari S, Chatterjee S, Alam J, Scardina F and Greco V (2017) *Phys. Lett. B* **768** 260
- [5] Skokov V, Illarionov A Y and Toneev V (2009) *Int. J. Mod. Phys. A* **24** 5925
- [6] Voronyuk V, Toneev V D, Cassing W, Bratkovskaya E L, Konchakovski V P and Voloshin S A (2011) *Phys. Rev. C* **83** 054911
- [7] Cassing W and Bratkovskaya E L (2008) *Phys. Rev. C* **78** 034919
- [8] Cassing W and Bratkovskaya E L (2009) *Nucl. Phys. A* **831** 215
- [9] Bratkovskaya E L, Cassing W, Konchakovski V P and Linnyk O (2011) *Nucl. Phys. A* **856** 162
- [10] Toneev V D, Voronyuk V, Kolomeitsev E E and Cassing W (2017) *Phys. Rev. C* **95** 034911
- [11] Oliva L, Moreau P, Voronyuk V and Bratkovskaya E (2019) arXiv:1909.06770 [nucl-th]
- [12] Poskanzer A M and Voloshin S A (1998) *Phys. Rev. C* **58** 1671
- [13] Adamczyk L *et al.* [STAR Collaboration] (2018) *Phys. Rev. Lett.* **120** 062301